THE JOURNAL OF BIOLOGICAL CHEMISTRY
Vol. 257, No. 17, Issue of September 10, pp. 10069-10080, 1982
Printed in U.S.A.

The Two-way Flux of Cationic Amino Acids across the Plasma Membrane of Mammalian Cells Is Largely Explained by a Single Transport System*

(Received for publication, January 18, 1982)

Morris F. White‡ and Halvor N. Christensen§

From the Department of Biological Chemistry, The University of Michigan Medical School, Ann Arbor, Michigan 48109

We show in this report that the inward and outward transport of cationic amino acids through the plasma membrane of cultured fibroblasts and HTC cells is mediated mostly by a single saturable transport system, here designated y^+. The kinetic behavior of System y^+ can be accounted for by the alternating generation of at least two conformational states, one on each side of the plasma membrane. No predictions are made as to the mechanism of these carrier oscillations. The saturable flux of cationic amino acids in both directions is strongly increased by the presence of competing substrates on the side of the membrane opposite to the measured flux. The kinetic parameters describing these interactions vary as predicted by the classical mobile carrier hypothesis. These observations support the homogeneity of mediated cationic amino acid transport. Our results do not exclude other small flux contributions by a minor, apparently passive nonsaturable migration in each direction. The mediated arginine influx is half-maximally saturated at an external substrate concentration 1/10 to 1/20 as high as the apparent intracellular concentration that half-maximally saturates efflux. The maximum flux through System y^+ attained by raising the substrate concentration to a saturating level is about equal in the two directions. The test amino acids accumulate 5- to 20-fold into HTC cells and human skin fibroblasts, findings which are consistent with the kinetic asymmetry of System y^+.

Membrane transport systems in higher animals serve physiologically for exodus of nutrients from as well as for entry of nutrients into a particular tissue (1, 2). This two-way service may alternate during the diurnal cycle, as for amino acids flowing to and from the liver in proceeding from the postprandial to the postabsorptive phase (3). For some tissues, a given amino acid may show a continuous net outward flow which is balanced presumably by a net inward flow of precursor molecules (4). The net flow of branched chain amino acids to muscle and of glutamine and alanine away from muscle provides examples. Arginine flows illustrate the complexities that may arise; rat muscle (5) and kidney (6) release net quantities of arginine into the bloodstream, whereas, in man, the splanchnic tissues in the aggregate take up only relatively small amounts of arginine (4). Rats grow, albeit slowly, when fed an arginine-free diet (7), suggesting that adequate arginine nutrition can occur through the interorgan flows. Studies of amino acid transport have tended to give only minor attention to the routes of amino acid exodus from cells because of a misconception that efflux usually represents physical leakage (8). In addition to influx, mediated efflux should prove to be an important site of metabolic regulation.

We use the occurrence of *trans*-stimulation of the arginine fluxes across the plasma membrane of cultured fibroblasts (9) and a hepatoma cell line, HTC (10), to show that the major part of the inward and outward movements of cationic amino acids occurs by System y^+. The two fluxes of arginine and its analogs are well characterized by the iso uni uni velocity equation (11) which describes the operation of the classical mobile carrier (12) for a single substrate, as diagrammed in Fig. 1. The correspondence of our results to this classical model does not yet necessarily exclude other kinetic explanations (13, 14). Our analysis attributes the phenomenon of *trans*-stimulation to accelerative counterflow (15) which results from the direct mass action between substrates and transport components at each membrane surface rather than from an indirect modulation, for example, by allosteric phenomena. System y^+ catalyzes the asymmetric partition of substrates by introducing an apparent directional asymmetry between their inward and outward flows.

In the ordinary situation encountered with neutral amino acids where two or more parallel membrane systems mediate the flows of a nutrient (16), it is unlikely that a single system participates to exactly the same degree for entry and exodus (1, 17). Each system operates in two directions, but to varying degrees under physiologic conditions. Here we show that the two-way flux of cationic amino acids via System y^+ serves for the major portion of uptake and release of reactive solutes by the test cells. For the physiologic context, participation by other agencies, including the so-called nonsaturable routes, has not been wholly excluded, but may be insignificant. Transport satisfactorily described in one direction by a single set of kinetic parameters may prove heterogeneous given that a second transport agency shows kinetic constants similar to the first (18). However, when the set of curves and parameters serve to describe consistently the bidirectional flow and *trans*-stimulation observed for a series of analogs, the support for homogeneity is greatly strengthened.

MATERIALS AND METHODS[1]

Human fibroblasts (19) and HTC cells (Morris 7288C, supplied by

* This work has been supported by Grant HD01233 from the Institute of Child Health and Human Development, National Institutes of Health, United States Public Health Service. The costs of publication of this article were defrayed in part by the payment of page charges. This article must therefore be hereby marked "*advertisement*" in accordance with 18 U.S.C. Section 1734 solely to indicate this fact.

‡ Present address, Joslin Diabetes Center, Boston, MA 02215.

§ To whom correspondence should be addressed.

[1] Portions of this paper (including part of "Materials and Methods," Equations 4-17, and additional references) are presented in miniprint at the end of this paper. Miniprint is easily read with the aid of a standard magnifying glass. Full size photocopies are available from

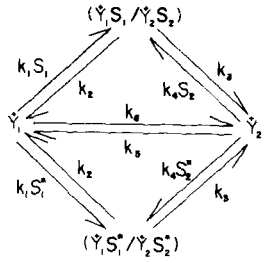

FIG. 1. **A schematic representation of the mobile carrier.** The iso uni uni reaction describes membrane transport of the extracellular (S_1) and intracellular (S_2) substrates. Radioactively labeled solute is indicated with an asterisk. The membrane component of System y^+, namely y_v^+, interacts with the substrate outside the cell and inside the cell. *Even-numbered subscripts* describe a cycle of efflux and *odd-numbered subscripts* describe a cycle of influx.

Dr. Thomas D. Gelehrter, Department of Human Genetics, University of Michigan) (20) were cultured in Medium 199 (GIBCO) supplemented with 10% fetal calf serum and were prepared for transport assay as described previously (9, 10, 21). Prior to the kinetic measurements, the confluent monolayers of fibroblasts or HTC cells were washed twice and incubated for at least 2 h in aminoacid-free modified Earle's balanced salt solution to deplete the endogenous amino acids (9). Then the cells were exposed to unlabeled or radioactive amino acids for selected time intervals. D-[U-^{14}C]3-*O*-Methylglucose (300 mCi/mmol), L-[2,3-^{14}C]arginine (333 mCi/mmol), L-[^{14}C]lysine (343 mCi/mmol), and L-[2,3-^{3}H]ornithine (15.4 Ci/mmol) were obtained from New England Nuclear. 4-Amino-1-[1-^{14}C]guanylpiperidine-4-carboxylic acid (22) and L-[2,3-^{3}H]homoarginine (23) were synthesized in our laboratory. All other materials used were as described previously (9, 10). Details of particular experimental manipulations are provided in the table or figure legends. Initial amino acid uptake was estimated by 20- to 30-s incubations with radioactively labeled substrates using previously described techniques (21). These time intervals were short enough to approximate the initial rate of uptake. The intracellular contents of rapidly metabolizable amino acids obtained after incubations of 30 to 60 min were determined chromatographically with an amino acid analyzer as previously described (9). The accumulation of slowly metabolized substrates, such as arginine and homoarginine, or of substrates incubated in the presence of 2 mM aminooxyacetate (Sigma), a compound that inhibits certain steps in amino acid metabolism (24), were assayed radiochemically. Efflux was approximated by loading the monolayers to a selected intracellular steady state concentration with a labeled amino acid and by subsequently measuring the initial rate of escape into EBS.[2] Initial exit was always measured during time intervals yielding less than 20% loss of the initial cellular content of the test amino acid.

The intracellular water volume used to estimate the intracellular substrate concentration was approximated by the method of Kletzien *et al.* (25) to be 4.0 μl of $H_2O \cdot mg^{-1}$ of protein for fibroblasts (9) and 4.6 μl of $H_2O \cdot mg^{-1}$ of protein for HTC cells (10).

Numerical analysis of initial velocity kinetic curves was carried out using FORTRAN programs described by Cleland (26) which apply the nonlinear Gauss-Newton least squares method to data described by the following general equations:

$$\log v = \log\left(\frac{V_{max}\cdot[S]}{K_m + [S]} + K_d\cdot[S]\right) \quad (1)$$

$$v = \frac{V_{max}\cdot[S]\cdot(1 + [P]/K_{ID})}{K_m(1 + [P]/K_{IS}) + [S](1 + [P]/K_{IN})} \quad (2)$$

$$v = \text{constant}\left(\frac{(1 + S/K_{IN})}{(1 + S/K_{ID})}\right) \quad (3)$$

the Journal of Biological Chemistry, 9650 Rockville Pike, Bethesda, MD 20814. Request Document No. 82M-104, cite the authors, and include a check or money order for $3.20 per set of photocopies. Full size photocopies are also included in the microfilm edition of the Journal that is available from Waverly Press.

[2] The abbreviations used are: EBS, Earle's balanced salt solution; AOA, aminooxyacetate; GPA, 4-amino-1-guanylpiperidine-4-carboxylic acid; BCH, the racemic 2-aminoendobicyclo[2.2.1]heptane-2-carboxylic acid.

The specific equations describing the kinetic model shown in Fig. 1 are developed in miniprint. The corresponding kinetic parameters are defined in Table 1.

RESULTS

Arginine Countertransport in Human Fibroblasts and HTC Cells—Human fibroblasts were incubated with various concentrations of unlabeled arginine for 40 min. The range of intracellular concentrations obtained by this treatment was determined from parallel experiments using labeled arginine. Arginine metabolism was not detectable during this time interval (9); the accumulated arginine measured chemically with the amino acid analyzer agreed within 10% with the value determined radiochemically. Influx of [^{3}H]arginine between 0.005 and 1.0 mM was estimated from 30-s incubations, and the kinetic parameters derived by fitting the data obtained at each apparent intracellular arginine concentration to Equation 1 are provided in Table II. The values of V^1_{obs} increased significantly as the apparent intracellular arginine concentration, [Arg_2], increased. Small increases were noted in K^1_{obs}; the nonsaturable component for entry, $K_d{}^1$, displayed small fluctuations. The Lineweaver-Burk plots describing these data are shown in Fig. 2*A*, and similar results obtained from an identical experiment with HTC cells are shown in Fig. 2*B*.

Typical replots of $1/V^1_{obs}$ (Fig. 3*A*) and K^1_{obs}/V^1_{obs} (Fig. 3*B*) are shown for arginine influx into fibroblasts. These kinetic parameters are hyperbolically related to the intracellular arginine concentration as predicted from Equations 8a and 9a. A double reciprocal plot of these data shown in the *insets* to Fig. 3, *A* and *B*, yields the linear relations expected for catalysis by a single agency. In this example, the hyperbolic dependence of $1/V^1_{obs}$ and K^1_{obs}/V^1_{obs} for [^{3}H]arginine entry on the intracellular arginine concentration, [Arg_2], can be used to estimate the apparent values of the intracellular Michaelis constants, $K_m{}^2$, $K_v{}^2$, and $K_c{}^2$ (see Table I). Two possible approaches for analyzing these results involve fitting the measured kinetic curves shown in Fig. 3, *A* and *B*, to Equation 3 or interpreting graphically the linear plots of the data shown in the *insets* to Fig. 3. We chose a more direct route by fitting the measured influx data, after deducting the nonsaturable component, into the complete iso uni uni velocity equation for influx (Equation 6). This method calculates all the kinetic parameters directly from a least squares analysis (Equation 2) and also provides estimates of precision. The kinetic parameters obtained after fitting the data to Equation 2 for two separate experiments with human fibroblasts and a single experiment with HTC cells are provided in Table III.

A similar experiment in which [^{3}H]arginine influx into fibroblasts was measured after loading fibroblasts with unlabeled homoarginine is shown in Table IV. The calculated kinetic constants are very similar to those listed in Table III for experiments with arginine. The apparent ratio of the zero-*trans*[3] Michaelis constants, $K_m{}^2/K_m{}^1$, from the three experiments with fibroblasts is about 24, whereas this value is near 7 in HTC cells. These observations emphasize the apparent kinetic asymmetry of System y^+ operation and are consistent with the accumulation of arginine and homoarginine observed for fibroblasts (Fig. 4 and Ref. 9) and for HTC cells (10). Similar results have been reported for the Ehrlich cell (27). The distribution ratio for cationic amino acids is probably determined to a large extent by this asymmetry. The question that remains unresolved is by what mechanism this asymmetry is produced. The influence of the membrane potential will be discussed later.

[3] Zero-*trans* influx ($K_m{}^1$, V^1_{max}) and efflux ($K_m{}^2$, V^2_{max}) are ideal experimental situations in which the initial velocity of substrate flux is measured in the absence of transport-reactive compounds inside or outside of the cell, respectively.

TABLE I

Kinetic parameters and molecular rate constants for the iso uni uni velocity equation

Kinetic Parameters[1] [2] [3]	Definition	Molecular Rate Constants	Kinetic Identities	Stein's Nomenclature
V^1_{max}	Maximum zero-*trans* influx	$\frac{k_3k_5}{k_3+k_5}$	$V^{ss}_{max}\bullet K^2_c/K^2_v$	$1/R_{12}$
V^2_{max}	Maximum zero-*trans* efflux	$\frac{k_2k_6}{k_2+k_6}$	$V^{ss}_{max}\bullet K^1_c/K^1_v$	$1/R_{21}$
V^{ss}_{max}	Maximum infinite-*trans* or steady-state flux	$\frac{k_2k_3}{k_2+k_3}$	$V^1_{max}\bullet K^2_v/K^2_c$ $V^2_{max}\bullet K^1_v/K^1_c$	$1/R_{ee}$
V^{oo}_{max}	Maximum empty carrier flux	$\frac{k_5k_6}{k_5+k_6}$	$V^1_{max}\bullet K^1_c/K^1_m$ $V^2_{max}\bullet K^2_c/K^2_m$	$1/R_{oo}$
K^1_m	Michaelis constant zero-*trans* influx	$\frac{(k_2+k_3)(k_5+k_6)}{k_1(k_3+k_5)}$	$K^1_v\bullet K^2_m/K^2_v$ $K^1_s\bullet K^2_c/K^2_v$	$K_{12}\bullet R_{oo}/R_{12}$
K^2_m	Michaelis constant zero-*trans* efflux	$\frac{(k_2+k_3)(k_5+k_6)}{k_4(k_2+k_6)}$	$K^2_v\bullet K^1_m/K^1_v$ $K^2_s\bullet K^1_c/K^1_v$	$K_{21}\bullet R_{oo}/R_{21}$
K^1_s	Michaelis constant steady-state influx	$\frac{(k_5+k_6)k_2}{k_1k_5}$	$K^1_m\bullet K^2_v/K^2_c$	$K_{12}\bullet R_{oo}/R_{ee}$
K^2_s	Michaelis constant steady-state efflux	$\frac{(k_5+k_6)k_3}{k_4k_6}$	$K^2_m\bullet K^1_v/K^1_c$	$K_{21}\bullet R_{oo}/R_{ee}$
K^1_v	Michaelis constant infinite-*trans* influx	$\frac{k_2+k_6}{k_1}$	$K^1_m\bullet K^2_v/K^2_m$	$K_{12}\bullet R_{21}/R_{ee}$
K^2_v	Michaelis constant infinite-*trans* efflux	$\frac{k_3+k_5}{k_4}$	$K^2_m\bullet K^1_v/K^1_m$	$K_{21}\bullet R_{12}/R_{ee}$
K^1_c	Michaelis constant countertransport	$\frac{k_6(k_2+k_3)}{k_1k_3}$	$V^2_{max}\bullet K^1_v/V^{ss}_{max}$	K_{12}
K^2_c	Michaelis constant countertransport	$\frac{k_5(k_2+k_3)}{k_2k_4}$	$V^1_{max}\bullet K^2_v/V^{ss}_{max}$	K_{21}
K_{eq}	Distribution ratio	$\frac{k_1k_3k_5}{k_2k_4k_6}$	K^2_c/K^1_c	K_{21}/K_{12}

[1] K^1_{obs} and K^2_{obs} are the observed Michaelis constants for influx and efflux, respectively.

[2] V^1_{obs} and V^2_{obs} are the observed kinetic parameters describing the maximum saturable influx and efflux, respectively.

[3] K^1_d and K^2_d are the observed kinetic parameters describing the nonsaturable components for influx and efflux, respectively.

At saturating internal solute concentrations, the value of V^1_{obs} for influx should equal V^{ss}_{max} or, equivalently, $V^1_{max}\cdot K_v^2/K_c^2$. This relation of kinetic parameters indicates that the maximum *trans*-stimulation of influx is determined by the ratio, K_v^2/K_c^2, which for arginine transport is about 7 in fibroblasts and 10 in HTC cells (Table III).

Intracellular arginine or homoarginine increased the apparent values of K^1_{obs} for uptake of arginine although not as

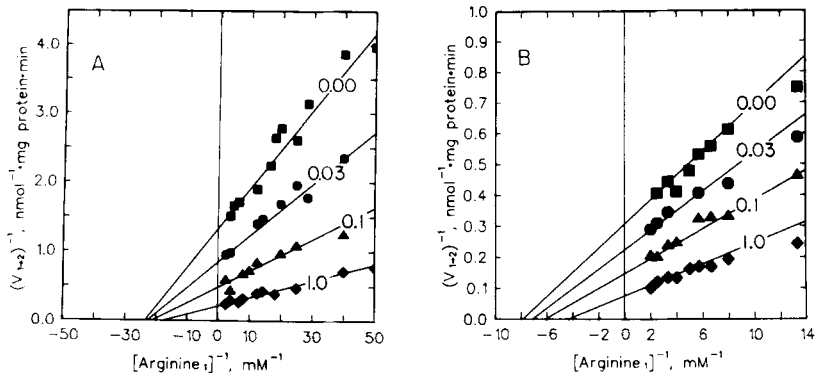

FIG. 2. **Lineweaver-Burk plots of arginine influx into fibroblasts (*A*) and HTC cells (*B*).** Following amino acid depletion, the cells were incubated for 40 min with the indicated concentrations (millimolar) of unlabeled arginine. After this incubation period, the monolayers were quickly washed (<4 s) with amino acid-free EBS at 37 °C. Influx ($V_{1\to2}$) was estimated from 30-s (fibroblasts) or 20-s (HTC cells) incubations with [^{3}H]arginine between 0.005 to 1.0 mM. The nonsaturable component for fibroblasts (4.0 nmol·mg^{-1} of protein·min^{-1}·mM^{-1}) and for HTC cells (0.3) has been subtracted from these data.

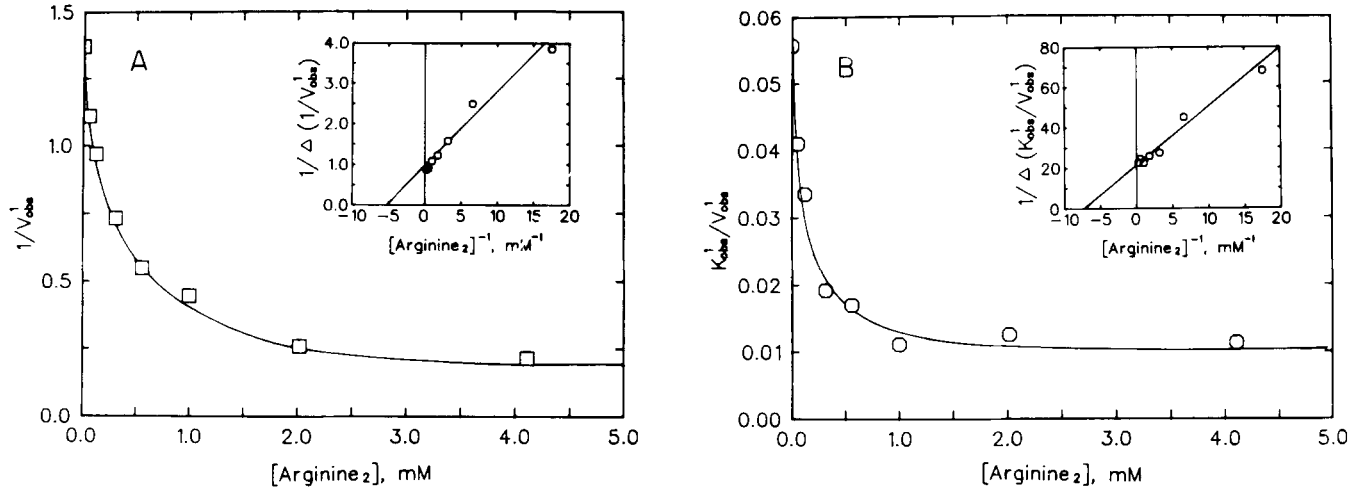

FIG. 3. **Replots of the intercepts (*A*) and slopes (*B*) from the Lineweaver-Burk plots in Fig. 2*A* for arginine influx into fibroblasts.** The apparent intracellular arginine concentration, [Arg$_2$], was estimated by incubating a parallel population of cells with the labeled amino acid. The internal water volume of 4 μl/mg of protein was used to calculate the intracellular amino acid concentrations. The data presented in *A* and *B* are plotted according to Equations 8a and 9a, respectively, whereas the *insets* show the linear transformations of the same data described by Equations 8b and 9b, respectively.

dramatically as the detected stimulation of V^1_{obs}. This phenomena, most apparent in HTC cells (Fig. 2*B*), has been emphasized by Heinz (15). The ratio of $K_v{}^1$ to $K_m{}^1$ is a measure of the maximum increase of K^1_{obs} and has a value of about 2 for fibroblasts and 3.5 for HTC cells. This ratio of infinite-*trans*[4] to zero-*trans* Michaelis constants for entry is equal to the analogous relation for efflux, $K_v{}^2/K_m{}^2$, indicating that proportional increases in K^1_{obs} for uptake and K^2_{obs} for exit are produced by substrates on the opposite side of the membrane (11). The values of the observed Michaelis constants for influx and efflux depend upon the substrate distribution at the two faces of the membrane in a way that is predictable from the carrier hypothesis.

Countertransport of Diamino Acids by System y$^+$ in Fibroblasts—Studies of lysine and ornithine countertransport are complicated by the occurrence of considerable intracellular metabolism of these solutes during the incubation intervals. This problem was minimized in either of two ways. First, the amino acid analyzer was used to estimate chemically the cellular steady state concentration of lysine or ornithine, and second, for the case of lysine, AOA was used to inhibit B_6-dependent metabolism (24). AOA eliminated observable catabolism of lysine and ornithine during a 40-min incubation interval (Fig. 5). The kinetic parameters for lysine and ornithine influx obtained from experiments analogous to those outlined for arginine are shown in Table V. The behavior of these amino acids is similar to that seen for the metabolism-resistant guanidino analogs (Tables III and IV). The apparent value of V^1_{obs} for entry is increased maximally about 6-fold ($K_v{}^2/K_c{}^2 = 6$) by intracellular substrates. The ratios of the opposed zero-*trans* Michaelis constants, $K_m{}^2/K_m{}^1$, are smaller (Lys, 6; Orn, 12) than the values observed with arginine and homoarginine although an apparent asymmetry is observed. Fig. 6 shows that intracellular BCH has no effect on lysine uptake, whereas internal arginine stimulates lysine influx. These results re-emphasize the earlier conclusions that System y$^+$ mediates the flux of both diamino acids and arginine analogs (9, 10) and that this sodium-independent mediation is separate from any contribution by sodium-independent System L. [^{3}H]BCH influx into fibroblasts is Na$^+$-independent and is stimulated by previously accumulated unlabeled BCH (data not shown). The flux of BCH is well described by the iso uni uni velocity equation which demonstrates a homogeneity owing to a specific interaction of BCH with System L in fibroblasts (28, 29).

Lysine, ornithine, and particularly their lower homologs show tendencies to be transported into cells to some extent as zwitterionic forms through interactions with neutral amino acid transport systems (28, 30, 31). This complicating circumstance together with the rather higher nonsaturable component of uptake shown by lysine and ornithine have led us to emphasize the more unequivocally cationic guanidino amino acids in our appraisal of the two-way role of System y$^+$ for transport. Nevertheless, results reported here and previously

[4] Infinite-*trans* influx ($K_m{}^1$, V^{ss}_{max}) and efflux ($K_c{}^2$, V^{ss}_{max}) are ideal experimental situations in which the initial velocity of substrate flux is measured in the presence of saturating concentrations of transport reactive compounds inside or outside of the cell, respectively.

TABLE II

The effect of intracellular arginine on the kinetic parameters for arginine influx into fibroblasts

The kinetic constants for [^{3}H]arginine uptake were determined in human fibroblasts during a 30-s time interval over a concentration range of 0.005 to 1.0 mM. Prior to the kinetic experiment, the cells were incubated in aminoacid-free EBS for 2 h to deplete endogenous amino acids. The quantity of arginine loaded into the cells was estimated by measuring the accumulation of [^{14}C]arginine in parallel experiments. The near absence of endogenous lysine and ornithine was verified with the amino acid analyzer. Concentrations of arginine were calculated radiochemically assuming an intracellular water volume of 4 $\mu l \cdot mg^{-1}$ of protein. The kinetic parameters ± S.E. were determined by fitting the data to Equation 1.

$[Arg_2]$	K^1_{obs}	V^1_{obs}	K^1_{obs}/V^1_{obs}	$K_d{}^1$
mM	*mM*	*nmol·mg^{-1} protein·min^{-1}*	*nmol^{-1}·mg protein·min·mM*	*nmol·mg^{-1} protein· min^{-1}·mM^{-1}*
0.00	0.041 ± 0.008	0.73 ± 0.09	0.056 ± 0.006	4.0 ± 0.2
0.06	0.036 ± 0.008	0.90 ± 0.10	0.041 ± 0.004	5.0 ± 0.2
0.15	0.035 ± 0.007	1.0 ± 0.1	0.033 ± 0.004	5.0 ± 0.3
0.31	0.026 ± 0.004	1.4 ± 0.1	0.019 ± 0.002	3.7 ± 0.3
0.56	0.031 ± 0.007	1.8 ± 0.2	0.017 ± 0.002	3.8 ± 0.4
1.0	0.025 ± 0.014	2.2 ± 0.6	0.011 ± 0.004	4.8 ± 1.4
2.0	0.057 ± 0.013	3.9 ± 0.6	0.014 ± 0.002	4.9 ± 0.9
4.7	0.060 ± 0.009	4.6 ± 0.5	0.011 ± 0.001	4.3 ± 0.7
Average				4.4 ± 0.5

TABLE III

Kinetic parameters for inward arginine countertransport into fibroblasts and HTC cells

Human fibroblasts or HTC cells were incubated in aminoacid-free medium for 90 min and then incubated for 45 min with various concentrations (0.01, 0.03, 0.06, 0.10, 0.20, 0.40, and 1.0 mM) of unlabeled arginine. The internal arginine concentration was estimated radiochemically in separate experiments. The monolayers were quickly washed with EBS (<5 s) at 37 °C and were incubated for 30 s with [^{3}H]arginine between 0.005 and 1.0 mM. The kinetic parameters ± S.E. were determined by fitting the data to Equation 2. The nonsaturable component, 4.0 nmol·mg^{-1} of protein·min^{-1}·mM^{-1} (fibroblasts) or 0.3 nmol·mg^{-1} of protein·min^{-1} mM^{-1} (HTC cells), was subtracted from the data prior to the numerical analysis.

	Fibroblasts		HTC cells
	Experiment 1	Experiment 2	
V^1_{max} (nmol·mg^{-1} protein·min^{-1})	0.75 ± 0.06	1.5 ± 0.2	3.3 ± 0.2
$K_m{}^1$ (mM)	0.043 ± 0.007	0.031 ± 0.009	0.13 ± 0.02
$K_m{}^2$ (mM)	1.2 ± 0.3	0.8 ± 0.2	0.9 ± 0.2
$K_v{}^1$ (mM)	0.06 ± 0.01	0.07 ± 0.01	0.5 ± 0.2
$K_v{}^2$ (mM)	1.9 ± 0.3	1.9 ± 0.4	3.1 ± 0.6
$K_c{}^2$ (mM)	0.22 ± 0.03	0.35 ± 0.07	0.28 ± 0.03
$K_v{}^2/K_c{}^2$; V^{ss}_{max}/V^1_{max}	8.5 ± 0.9	5.3 ± 0.8	11 ± 2
$K_m{}^2/K_c{}^2$	6 ± 1	2.2 ± 0.7	3.1 ± 0.6
$K_v{}^2/K_m{}^2$	1.7 ± 0.3	2.4 ± 0.4	3.5 ± 0.8
$K_m{}^2/K_m{}^1$	28 ± 8	25 ± 9	7 ± 1

(9, 10) indicate that the influx and efflux of lysine and ornithine are primarily mediated by System y^+ in these cells.

Steady State Influx of Cationic Amino Acids—System y^+, like other biological catalysts, mediates the unidirectional fluxes of substrates even after a steady state distribution has been reached and when there is no net flux. The steady state influx[5] of arginine, ornithine, and homoarginine can be characterized in each case as the sum of a saturable and a nonsaturable component. Accordingly, the steady state influx of these substrates was fitted to Equation 1. Table VI lists the steady state kinetic parameters obtained and compares them with the expected values calculated from the kinetic constants measured from the inward countertransport experiments reported in Tables III–V. Agreement of the values for $K_s{}^1$ and V^{ss}_{max} measured by the steady state experiment with the ratios $K_m{}^1 \cdot K_v{}^2/K_c{}^2$ and $V^1_{max} \cdot K_v{}^2/K_c{}^2$, respectively, measured by a countertransport experiment indicates the consistency of our kinetic analysis and the validity of the iso uni uni reaction in this context. A comparison of the arginine influx curves obtained in the absence of intracellular arginine (approximately zero-*trans* influx), in the presence of a high concentration of intracellular arginine (approximately infinite-*trans* influx), and at the steady state is shown in Fig. 7. The shapes of these curves depend upon the distribution of substrate at the moment of the influx measurement. The apparent maximum influx for both the infinite-*trans* and steady state experiments, V^{ss}_{max}, is nearly identical as predicted from the iso uni uni velocity equation (31). The shapes of these two curves are different, however, owing to the inequality of K^1_{obs} under these

[5] Steady state influx ($K_s{}^1$, V^{ss}_{max}) and efflux ($K_s{}^2$, V^{ss}_{max}) are essentially isotope-exchange experiments in which the flow of labeled substrate is measured after the distribution of unlabeled substrates has reached a steady state at the same concentrations.

TABLE IV

Kinetic constants determined for homoarginine-stimulated arginine influx into human fibroblasts

Human fibroblasts were incubated in aminoacid-free medium for 90 min and then incubated for 45 min with various concentrations (0.01, 0.03, 0.06, 0.10, 0.20, 0.40, and 1.0 mM) of unlabeled homoarginine. The monolayers were quickly washed with EBS (<5 s) at 37 °C and were incubated with [^{3}H]arginine between 0.005 and 1.0 mM for 30 s. The kinetic parameters ± S.E. were determined by fitting the data to Equation 2. The average values of the nonsaturable component, 3.72 ± 0.7 nmol·mg^{-1} of protein·min^{-1}·mM^{-1}, were deducted from the data before the numerical analysis.

Kinetic parameter	Value
V^1_{max} (nmol·mg^{-1}protein·min^{-1})	0.52 ± 0.07
$K_m{}^1$ (mM)	0.04 ± 0.01
$K_m{}^2$ (mM)	0.8 ± 0.2
$K_v{}^1$ (mM)	0.08 ± 0.01
$K_v{}^2$ (mM)	1.4 ± 0.2
$K_c{}^2$ (mM)	0.17 ± 0.02
$K_v{}^2/K_c{}^2$; V^{ss}_{max}/V^1_{max}	9 ± 1
$K_m{}^2/K_c{}^2$	5 ± 1
$K_v{}^2/K_m{}^2$	1.7 ± 0.3
$K_m{}^2/K_m{}^1$	19 ± 7

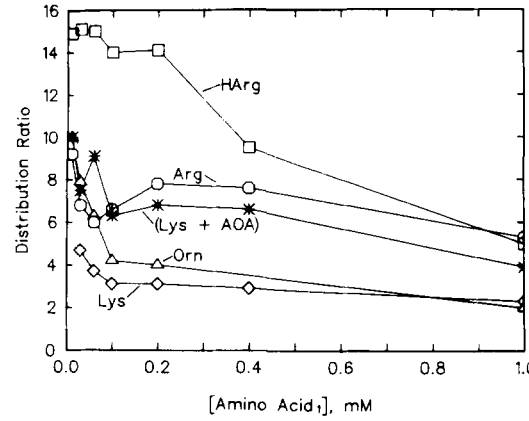

FIG. 4. **The effect of the concentration of extracellular cationic amino acids on their distribution ratios in human fibroblasts.** Fibroblasts were incubated with the indicated concentrations of unlabeled lysine (◇) or ornithine (△) in 75-cm^2 Corning flasks or [^{14}C]lysine (*), [^{3}H]arginine (○), or [^{3}H]homoarginine (□) in Costar cluster trays for 40 min. The experiment with [^{14}C]lysine also contained 2 mM *AOA*. The nonradioactive compounds were extracted with 75% ethanol and quantitated with an amino acid analyzer. The labeled compounds were extracted with 10% trichloroacetic acid and determined radiochemically. The intracellular water volume used to calculate the distribution ratios was assumed to be 4 $\mu l \cdot mg^{-1}$ of protein.

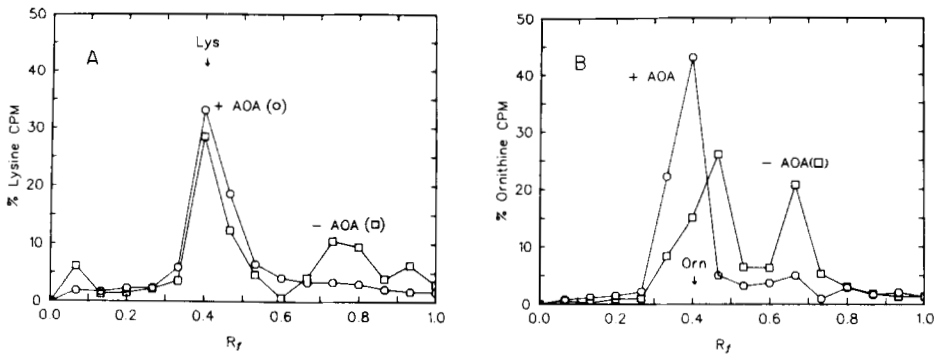

FIG. 5. **Thin layer chromatography of ornithine and lysine.** Cellulose thin layer chromatography of L-[U-^{14}C] lysine (*A*) and L-[U-^{3}H]ornithine (*B*) was obtained from ethanol extracts of fibroblasts incubated for 40 min in the presence (○) or absence (□) of 2 mM *AOA*.

TABLE V

Some kinetic parameters determined for inward lysine and ornithine countertransport in fibroblasts

Human fibroblasts were incubated in aminoacid-free medium for 120 min and then incubated for 40 min with various concentrations (0.01, 0.03, 0.06, 0.10, 0.20, 0.40, and 1.0 mM) of unlabeled lysine or ornithine. No AOA was used in the first experiment, in which the intracellular lysine concentration was measured in parallel experiments with the amino acid analyzer. In the second experiment, the cells were exposed to 2 mM AOA for 5 min before and also during incubation of the cells with [^{14}C]lysine. The internal lysine concentration was estimated radiochemically in this latter experiment. No AOA was used during incubation of the cells with ornithine. The internal ornithine level in the third experiment was estimated with data obtained from amino acid analysis. After these incubations, the monolayers were quickly washed with EBS (<5 s) at 37 °C and were incubated with [^{14}C]lysine or with [^{3}H]ornithine between 0.005 and 1.0 mM for 30 s. The kinetic parameters ± S.E. were determined by fitting the data to Equation 2. The nonsaturable component had an average value of 7.0 nmol·mg^{-1} of protein·min^{-1}·mM^{-1} for both trials of lysine uptake and 3.7 ± 0.7 for the experiment with ornithine.

Kinetic parameter	Lysine		Ornithine (−AOA)
	−AOA	+AOA	
V^1_{max} (nmol·mg^{-1}protein·min^{-1})	0.51 ± 0.06	0.4 ± 0.04	1.09 ± 0.04
$K_m{}^1$ (mM)	0.017 ± 0.006	0.06 ± 0.01	0.071 ± 0.006
$K_m{}^2$ (mM)	0.11 ± 0.04	0.31 ± 0.06	0.9 ± 0.2
$K_i{}^1$ (mM)	0.12 ± 0.06	0.07 ± 0.02	0.27 ± 0.08
$K_i{}^2$ (mM)	0.76 ± 0.09	0.41 ± 0.05	3.4 ± 0.7
$K_c{}^2$ (mM)	0.11 ± 0.03	0.08 ± 0.01	0.52 ± 0.06
$K_i{}^2/K_c{}^2$; V^{ss}_{max}/V^1_{max}	7.0 ± 0.8	5.0 ± 0.5	6.5 ± 0.8
$K_m{}^2/K_c{}^2$	1.0 ± 0.3	3.7 ± 0.7	1.7 ± 0.2
$K_i{}^2/K_m{}^2$	7.0 ± 2.2	1.4 ± 0.4	3.8 ± 0.7
$K_m{}^2/K_m{}^1$	7 ± 3	5 ± 1	12 ± 2

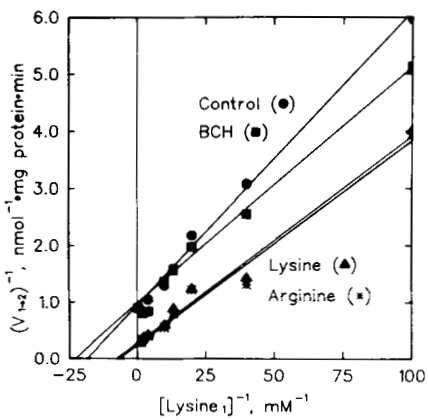

FIG. 6. ***Trans*-stimulation of lysine influx into fibroblasts.** Lineweaver-Burk plots are shown for 30-s lysine influx ($V_{1\to2}$) after 30-min incubations of fibroblasts in aminoacid-free EBS (●) or in EBS containing 10 mM levels of arginine (×), lysine (▲), or BCH (■). The monolayers were washed briefly (<4 s) with EBS at 37 °C immediately before the uptake. The average nonsaturable component of lysine influx ($K_d{}^1$ = 7.0 nmol·mg^{-1} of protein·min^{-1}·mM^{-1}) was determined by fitting the data to Equation 1. This value was insensitive to the presence of intracellular amino acid and has been subtracted from the data shown in this figure.

conditions, namely, $K_s{}^1 > K_v{}^1$. This result should always occur for a transport system displaying accelerative countertransport. Furthermore, the ratios of kinetic parameters measured during steady state ($V^{ss}_{max}/K_s{}^1$) and zero-*trans* ($V^1_{max}/K_m{}^1$) influx were equal, whereas the values determined from the infinite-*trans* ($V^{ss}_{max}/K_v{}^1$) influx experiment were significantly larger. These relations, shown also for a number of hepatoma cell lines (10), are predicted from the iso uni uni velocity equation and support the argument that System y$^+$ operates as a mobile carrier in two directions.

In the intact organism, solute flux would normally occur at an apparent steady state so that the observed Michaelis constants governing the influx (K^1_{obs}) and efflux (K^2_{obs}) are equal to $K_s{}^1$ and $K_s{}^2$, respectively, rather than to the corresponding zero-*trans* parameters, $K_m{}^1$ and $K_m{}^2$. $K_m{}^1$ for cationic amino acid entry is roughly one-sixth to one-seventh of the value of $K_s{}^1$ in human fibroblasts (Table VI) and in a number of hepatoma cell lines (see Table VI in Ref. 10). This distinction between $K_m{}^1$ and $K_s{}^1$ is important because the aggregate physiologic concentration of arginine, lysine, and ornithine is about 0.26 mM, implying that System y$^+$ is ordinarily operating well below saturation at the physiologic steady state (33). However, at low cellular levels possibly resulting from rapid metabolism, the system may be largely saturated (Fig. 7).

Efflux of Arginine from Human Fibroblasts and HTC Cells—The loss of [^{3}H]arginine into EBS containing 10 mM arginine (Fig. 8*B*) is accelerated over the loss into initially aminoacid-free EBS (Fig. 8*A*). Standard kinetic plots and the corresponding kinetic parameters for arginine efflux from fibroblasts and HTC cells are shown in Fig. 9, *A* and *B*, respectively. Within the apparent internal concentration interval of 0.02 to 20 mM, the efflux of arginine corresponds to the sum of a saturable and a nonsaturable component, an observation which is analogous to the findings for influx (9). The initial velocity of exodus (the efflux) measured during a 1-min incubation of fibroblasts in aminoacid-free medium was fitted to Equation 1. The apparent value obtained for $K_m{}^2$, 0.9 ± 0.3 mM, agreed remarkably well with the values determined from the influx countertransport experiments (Table III). A similar correspondence was seen for HTC cells (compare Fig. 9*B* and Table III). These results indicate that the carrier hypothesis applied to System y$^+$ can explain consistently the two-way flux of cationic amino acids in human fibroblasts and HTC cells. In both cell types tested, V^2_{max} is slightly larger than V^1_{max}, but this difference may not be significant and may arise from the greater technical difficulty in measuring efflux. From the results presented in this section and in Table III, the magnitude of the theoretical distribution ratio for arginine, K_{eq}, resulting from the asymmetry of System y$^+$ can be cal-

culated from Equation 11 to have a value of about 20 in fibroblasts and 10 in HTC cells. These values arise primarily from an asymmetry in K_m.

Measurement of efflux at internal solute concentrations much lower than K_m^2 permits direct estimation of the extracellular kinetic parameters K_c^1 and K_m^1 and also of the effect of external substrate on the value of V^2_{obs}/K^2_{obs}. These variables are related by Equation 17a. We will call this a measurement of first-order efflux because the apparent initial rate of exodus after deducting the nonsaturable flux is proportional to V^2_{max}/K_m^2. Fig. 10 shows that the value of V^2_{obs}/K^2_{obs} estimated from the ratio of intracellular [^{3}H]arginine ($[Arg_2] \ll K_m^2$) to the efflux of [^{3}H]arginine ($[Arg_2]/V_{2\to1}$) decreased hyperbolically as the external arginine concentration increased. The linear replot of these data according to Equation 17b shown in the *inset* to Fig. 10 verifies this conclusion. The efflux of [^{3}H]arginine, $V_{2\to1}$, has been corrected in this case for the nonsaturable component assuming that the value of K_d^2 for efflux measured from the experiment in Fig. 9*A*, 0.3 nmol·mg^{-1} of protein·min^{-1}·mM^{-1}, was unaffected by the external arginine concentration. This assumption is plausible because at no time was the value of K_d^1 for influx affected by *trans*-substrates (Table II). The data were fitted to Equation 3 and yielded a value of V^2_{max}/K_m^2, which was close to that determined directly from the efflux experiments (Fig. 9*A*). At infinite arginine concentration outside the cell, V^2_{obs}/K^2_{obs} (specifically, V^{ss}_{max}/K_v^2) was 4.1 ± 0.2 nmol·mg^{-1} of protein·min^{-1}·mM^{-1}. From the value of K_v^2 measured by the countertransport experiment (Table III), V^{ss}_{max} was calculated to be 7.8 nmol·mg^{-1} of protein·min^{-1}, a value consistent with the other estimates obtained from influx experiments (Table VI).

The assessment of K_m^1 obtained by the first-order efflux experiment, 0.030 ± 0.005 mM, is close to the value measured directly from the influx experiments shown in Table III and in previous reports (9). The value of K_c^1 was 0.013 mM (Fig. 10), from which a theoretical distribution ratio, K_c^2/K_c^1, is calculated to be about 21 at infinite dilution and in the absence of other transport pathways. This value of K_{eq} is identical with that calculated from estimates of V_{max} and K_m for influx and efflux discussed above. This correspondence summarized by Equation 11a is predicted from the iso uni uni velocity equation (11).

Analysis of lysine and ornithine efflux at very low intracellular concentrations has not been possible owing to the rapid metabolism of these substrates.

The Asymmetric Flux of 4-Amino-1-guanidinopiperidine-4-carboxylic Acid by System y$^+$—The failure of GPA to *trans*-stimulate arginine influx (Fig. 11*A* and Refs. 8 and 9) and the corresponding absence of arginine-stimulated GPA exodus can be interpreted by the kinetic analysis presented in this report. Because K_m^1 for GPA uptake into fibroblasts is near 1 mM (9), the value of K_m^2 must be at least 10-fold higher and is probably larger. The low concentration of GPA relative to K_m^2 would cause GPA to react weakly at the inner surface of the membrane; V^2_{max}/K_m^2 could be less than 0.1 nmol·mg^{-1} of protein·min^{-1}·mM^{-1}, assuming a V^2_{max} of the same order as for arginine. Therefore, a measurable acceleration of carrier reorientation would probably not be observed. Fig. 11*B* confirms that external concentrations of GPA near K_m^1 stimulate arginine and homoarginine exodus but not the exit of GPA. Corresponding asymmetry in the *trans*-effects of this and other paired amino acids have been noted in the Ehrlich cell (33), providing earlier support for System y$^+$ asymmetry.

TABLE VI

Kinetic parameters describing cationic amino acid influx at steady state

The apparent kinetic constants (K_s^1, V^{ss}_{max}) for the steady state influx of labeled amino acids were measured after 45-min incubations of fibroblasts with various concentrations of the unlabeled cognate amino acid. At this point, net flux presumably approaches zero and the solutions were replaced with buffer containing labeled amino acids at the same concentrations. Influx of [^{3}H]arginine was measured for 30 s and the resulting data were fitted to Equation 1. The nonsaturable components were identical with those values observed previously. For comparison, the ratios of the kinetic parameters determined by the countertransport experiment, $K_m^1 \cdot K_c^2/K_c^2$ ($=K_d^1$) and $V^1_{max} \cdot K_c^2/K_c^2$ ($=V^{ss}_{max}$), were computed from the values listed in Tables III–V.

Substrate	K_s^1	V^{ss}_{max}	$K_m^1 \cdot K_c^2/K_c^2$	$V^1_{max} \cdot K_c^2/K_c^2$
	mM	nmol·mg^{-1} protein·min^{-1}	mM	nmol·mg^{-1} protein·min^{-1}
Arginine	0.31 ± 0.08	5 ± 1	0.26	7.6
Homoarginine	0.33 ± 0.03	7 ± 1		
Lysine			0.24	2.8
Ornithine	0.31 ± 0.09	5 ± 1	0.35	7.1

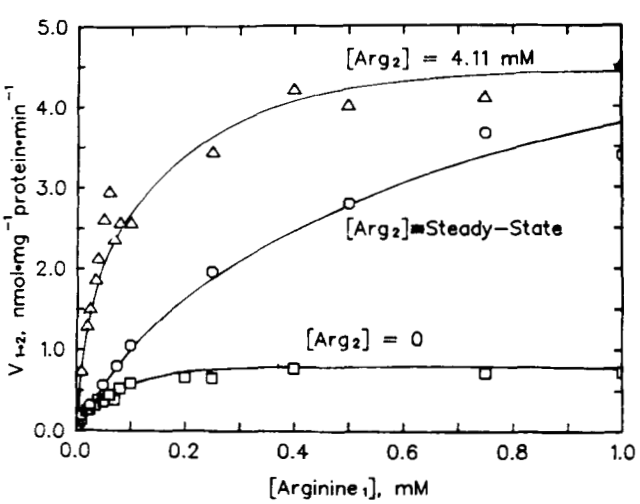

FIG. 7. **The effect of substrate distribution on the influx of [^{3}H]arginine.** After incubation of fibroblasts in EBS for 90 min, the cells were incubated for an additional 45 min with EBS (□) to obtain the zero-*trans* condition, with EBS containing 1 mM arginine (△) to approximate the infinite-*trans* condition, or with various concentrations of arginine corresponding exactly to those used for the influx measurements (○) to establish a steady state condition. The monolayers were quickly washed (<4 s) and influx of [^{3}H]arginine ($V_{1\to2}$) was estimated with 30-s uptakes. The nonsaturable components (approximately 3.5 nmol·mg^{-1} of protein·min^{-1}·mM^{-1} in each case) have been subtracted from the data shown in this figure.

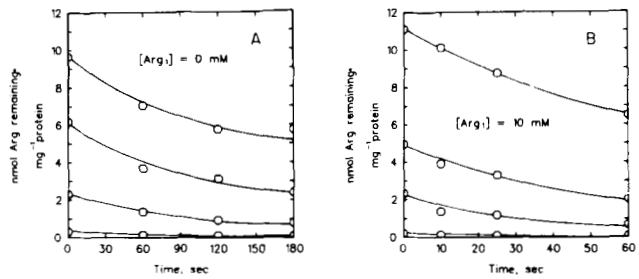

FIG. 8. **Time courses of arginine exodus into aminoacid-free and arginine-containing medium.** Fibroblasts were washed once and incubated in EBS for 60 min to deplete endogenous amino acid pools. The monolayers were then incubated with various concentrations (1.0, 0.75, 0.20, and 0.06 mM) of [^{3}H]arginine for 30 min to load the cells to different intracellular concentrations. Exodus was initiated by quickly washing the monolayers with EBS at 37 °C and then incubating the cells with 2 ml of fresh amino acid-free EBS (*A*) or EBS containing 10 mM arginine (*B*) for the indicated time intervals. The *data points* (○) represent averages of duplicate measurements of the [^{3}H]arginine remaining associated with the cells.

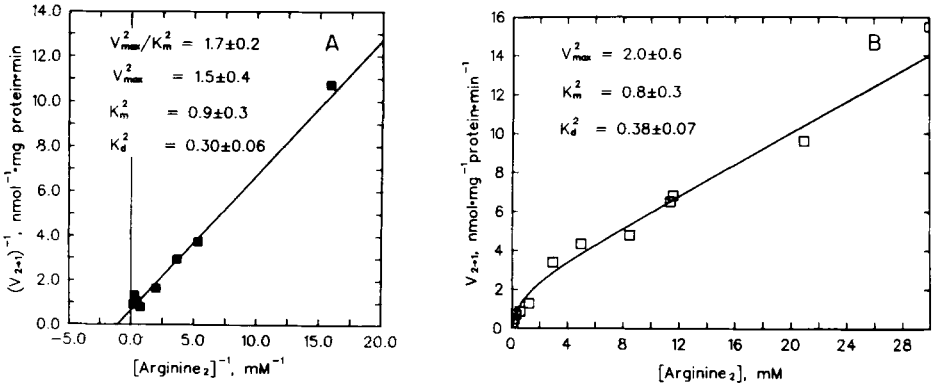

FIG. 9. **Kinetic curves describing the efflux of arginine from fibroblasts (*A*) and HTC cells (*B*).** Cells were incubated for 30 min with various concentrations (0.01 to 20 mM) of [^{3}H]arginine to attain apparent internal concentrations between 0.1 and 20 mM. Efflux ($V_{2\to1}$) was estimated as the difference between the initial concentration and the concentration of arginine remaining after a 1-min incubation (fibroblasts) or a 30-s incubation (HTC cells) in 1 ml of amino-acid-free EBS. The internal [^{3}H]arginine concentrations were taken as the average between these two values. Less than 25% of the initial amount of arginine was lost from the cells during the incubation interval. For clarity, all the data are not plotted in the figures although all data were fitted to Equation 1 to produce the lines. The nonsaturable component has been subtracted from the data in *A*. The corresponding kinetic parameters K_m^2 (mM), V^2_{max} (nmol·mg^{-1} of protein·min^{-1}), K_d^2 (nmol·mg^{-1} of protein·min^{-1}·mM^{-1}), and V^2_{max}/K_m^2 (nmol·mg^{-1} of protein·min^{-1}·mM^{-1}) are shown in the figures.

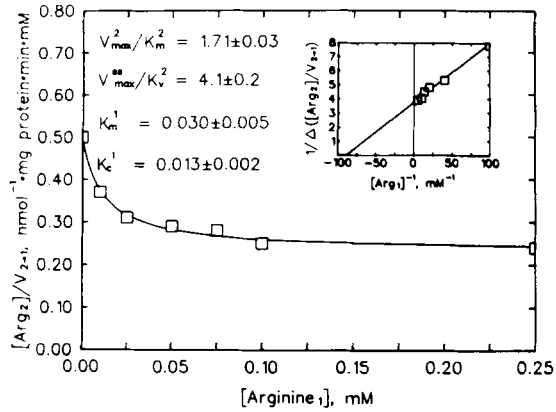

FIG. 10. **The effect of external arginine on the so-called mediated first-order efflux of [^{3}H]arginine.** Fibroblasts were incubated with 0.01 mM [^{3}H]arginine for 30 min to obtain an apparent internal concentration of 0.25 mM. Efflux ($V_{2\to1}$) was calculated from the difference between the [^{3}H]arginine initially present and the amount remaining after a 30-s incubation of the cells in EBS containing various concentrations of unlabeled arginine. The nonsaturable component determined for the efflux of arginine from fibroblasts (Fig. 9*A*) was subtracted from the measured efflux. The kinetic parameters K_c^1 (mM), K_m^1 (mM), and V^2_{max}/K_m^2 (nmol·mg^{-1} of protein·min^{-1}·mM^{-1}) were obtained by fitting the data to Equation 3. [S_2] was taken as 0.25 mM. These data are plotted according to Equations 17a and 17b (*inset*).

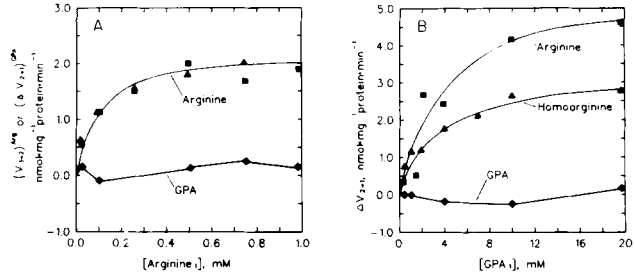

FIG. 11. **The asymmetry of GPA transport in fibroblasts.** *A*, [^{3}H]arginine influx ($(V_{1\to2})^{Arg}$) into fibroblasts estimated from 30-s uptakes following 30 min of incubation with EBS (▲) or with EBS containing 10 mM GPA (■). Also shown in this figure is the stimulated efflux of 3 mM [^{14}C]GPA ($(\Delta V_{2\to1})^{GPA}$) by extracellular arginine (◆). *B*, the effect of external GPA on the stimulation of efflux ($\Delta V_{2\to1}$) of [^{3}H]arginine (■), [^{3}H]homoarginine (▲), or [^{14}C]GPA (◆). The approximate internal concentration of the labeled amino acids was 3 mM.

These results provide qualitative support for the quantitative kinetic asymmetry of System y$^+$.

DISCUSSION

These studies demonstrate that the flow of cationic amino acids occurs predominantly by System y$^+$ and to lesser extents by nonsaturable components. Under physiologic conditions, the flux of cationic amino acids probably occurs at the steady state at which System y$^+$ is not even half-saturated ([Arg$_1$] + [Lys$_1$] + [Orn$_1$] < K_s^1). Thus, the portion of transport occurring through the mediated route relative to the nonsaturable routes can be calculated from the ratio $(V^1_{max}/K_m^1)/((V^1_{max}/K_m^1) + K_d^1)$ for influx or the ratio $(V^2_{max}/K_m^2)/((V^2_{max}/K_m^2) + K_d^2)$ for efflux. These calculations indicate that about 87 and 99% of arginine influx occurs by System y$^+$ in fibroblasts and HTC cells, respectively. Similarly, System y$^+$ mediates 85 and 87% of the arginine efflux measured from fibroblasts and HTC cells, respectively, Of course, as the arginine concentration rises to saturating levels, the relative contribution of System y$^+$ decreases because the nonsaturable uptake continues to increase linearly with concentration. Normally, System y$^+$ is significantly involved in the influx and efflux of cationic amino acids. However, kinetic data obtained with cultured rat hepatocytes suggests that System y$^+$ uptake is so small that most cationic amino acid uptake in these cells occurs by nonsaturable routes (10).

Many kinetic studies of solute transport have focused on the facilitated hexose transport system in human red blood cells. Wilbrandt (34) showed long ago that the nonaccumulating glucose transport system was asymmetric with respect to the plasma membrane. Karlish *et al.* (35) found the value of K_m^2 to be an order of magnitude larger than K_v^1, an observation which is consistent with the existence of an asymmetric transport system. Baker and Widdas (36) and Baker *et al.* (37) demonstrated with nontransportable inhibitors of glucose uptake that the asymmetry across the red blood cell membrane may be as high as 60-fold. These investigators extended the initial proposal of Geck (38) and suggested that nonaccumulating transport can occur through an asymmetric system without violating the second law of thermodynamics, given

only that $V^1_{max}/K_m{}^1 = V^2_{max}/K_m{}^2$. Equal and opposite asymmetry of V_{max} will counter differences in K_m across the membrane. Bloch (39) verified this relation in human red blood cells and Whitesell *et al.* (40) showed the same situation in rat thymocytes. Glucose transport has been shown to be directionally symmetric ($K_m{}^1 = K_m{}^2$, $V^1_{max} = V^2_{max}$) in rabbit erythrocytes (41), rat hepatocytes (42), Novikoff rat hepatoma cells (43, 44), and adipocytes (45). Asymmetric transport kinetics have been shown also for leucine and glycine flux in human (46) and pigeon (47) erythrocytes, respectively, whereas tryptophan flux in human red blood cells by System T was shown to be directionally symmetric (48). To conclude, the ratio V_{max}/K_m for translocation of neutral substrates must be equal in both directions for a passive transport system, but the individual kinetic parameters need not be equal across the membrane.

Our studies with System y^+ in fibroblasts and HTC cells have shown that, unlike the passive glucose transport system, $V^1_{max}/K_m{}^1$ is 10- to 20-fold greater than $V^2_{max}/K_m{}^2$. This asymmetry apparently results from differences between $K_m{}^1$ and $K_m{}^2$, whereas V^1_{max} and V^2_{max} are approximately equal (see Table III and Fig. 9, *A* and *B*). This asymmetry may represent the electrochemical equilibrium which occurs for cationic substrates when influenced by a membrane potential, inside negative. The theoretical distribution ratio, K_{eq}, calculated from the measured kinetic parameters is related to $\Delta\psi$ by Equation 11b. The values of 10 to 20 for K_{eq} are equivalent to −61 mV and −80 mV in HTC cells and fibroblasts, respectively. Villereal and Cook (50) measured values for the membrane potential of −47 to −24 mV in growing and confluent human fibroblasts, respectively. Others have shown that manipulation of the amino acid pool may cause the membrane potential of Ehrlich cells to reach −63 mV (51, 52). The observed distribution ratios of arginine, lysine, and ornithine shown in Fig. 4 could be explained by the membrane potential. Given the present state of knowledge, quantitative relations between the membrane potential and transport kinetic parameters are tentative (53). No direct evidence exists to indicate whether accumulation of solutes by System y^+ in fibroblasts or HTC cells occurs by primary or secondary active transport. Christensen and Handlogten (27) have suggested that intramembrane proton gradients may be coupled to the accumulation of diamino acids by Ehrlich cells.

The nonsaturable component of arginine efflux from fibroblasts, $K_d{}^2$, was about 1/12 of the corresponding parameter for influx, $K_d{}^1$. Under the usual assumption that this mode of migration is passive (54–56), this ratio would correspond to a transmembrane potential of −66 mV. In the HTC cells, the two opposed nonsaturable fluxes were not clearly different because the value of $K_d{}^1$ was 1/10 of the value measured in fibroblasts, whereas $K_d{}^2$ was about equal in both cell types. We cannot explain this behavior but only restate that the nonsaturable component does not necessarily refer to a single homogeneous mode of migration or to one that is the same for the two cell types.

GPA reacted poorly at the outer face of the plasma membrane of fibroblasts (9) and HTC cells (10) and reacted imperceptibly at the inner face of these cells. This behavior apparently results from a lower reactivity of the substrate with System y^+. The value of $K_m{}^1$ for GPA is at least 10-fold larger than comparable measurements for the naturally occurring cationic amino acids. It is likely that $K_m{}^2$ for GPA efflux is so high because of the directional asymmetry of System y^+ that it would only sluggishly stimulate arginine influx at reasonable concentration intervals. These observations with GPA support our claim that System y^+ operates asymmetrically.

TABLE VII

The relative flux of the System y^+ receptor site under certain limiting conditions of substrate saturation

The values of V^{00}_{max} were calculated from Equation 10a using the data presented in Tables II–V and a previous report (see Table VII in Ref. 10). We assumed that $V^1_{max} = V^2_{max}$ for all the substrates tested, in which case Equation 10a simplifies to Equation 10b.

$$1/V^{00}_{max} = 2(1/V^1_{max} - 1/2V^{ss}_{max})$$

V^{00}_{max} is the maximum flux of the unloaded carrier; V^1_{max} is the maximum flux of the carrier loaded only during influx; and V^{ss}_{max} is the maximum flux of the carrier saturated with substrate during influx and efflux. The data reported for the hepatoma lines McA-RH777 and McA-RH8994 were calculated from measurements reported elsewhere (10).

Substrate (outside/inside)	Cell type	V^{00}_{max}	V^1_{max}/V^{00}_{max}	$V^{ss}_{max}/V^{00}_{max}$
		nmol·mg⁻¹ protein·min⁻¹		
Arg/Arg	Fibroblasts	0.59	1.7	13
Arg/HArg[a]	Fibroblasts	0.28	1.8	16
Lys/Lys	Fibroblasts	0.25	1.8	11
Orn/Orn	Fibroblasts	0.59	1.8	12
Arg/Arg	HTC	1.7	1.9	21
Arg/Arg	McA-RH7777	0.15	1.9	61
Arg/Arg	McA-RH8994	0.13	1.9	18

[a] HArg, L-homoarginine.

In addition to the directional asymmetry, System y^+ displayed differential mobility of complexed and uncomplexed carriers. This characteristic is observed for transport by a number of systems although not detected for the fluxes of system L of pigeon red blood cells (49). V^{00}_{max}, the maximum flux of the carrier empty during influx and efflux, can be calculated from Equation 10b for cationic amino acid transport in fibroblasts and a number of hepatoma cells. This calculation is valid only if V^1_{max} and V^2_{max} are equal for the test substrates, as specifically found for arginine flux in HTC cells and fibroblasts. Table VII lists the calculated values of V^{00}_{max} and the corresponding ratios, V^1_{max}/V^{00}_{max} and $V^{ss}_{max}/V^{00}_{max}$. These calculations indicate for all substrates and cell types tested that the complete cycle of the carrier with a substrate bound only during influx (V^1_{max}) or efflux (V^2_{max}) is twice as fast as a cycle of the carrier empty in both directions (V^{00}_{max}). The flux of the carrier saturated with amino acid during influx and efflux (V^{ss}_{max}) is 10- to 60-fold faster than that of the empty carrier ($V^{ss}_{max}/V^{00}_{max}$). This magnitude of stimulation has been reported for other transport systems (44). System y^+ is not an obligatory exchanging system because flux of the empty carrier can occur ($V^{00}_{max} > 0$). However, movement of the empty carrier is the rate-limiting step in transport by System y^+.

Graff *et al.* (43) suggested that the directional mobilities of the loaded and unloaded carrier may provide a site of regulation for glucose transport in Novikoff hepatoma cells. They found the value of $V^{ss}_{max}/V^{00}_{max}$ (R_{00}/R_{ee} in terms of Lieb and Stein's nomenclature (32)) to vary from 7 to 1.5 although they did not understand why. This ratio was constant for cationic amino acids studied here (Table VII). Only the McA-RH7777 cell line showed a 3-fold larger value, an observation which may prove significant only after further study.

Finally, a note of caution must be added. The values of the intracellular kinetic parameters, $K_m{}^2$, $K_v{}^2$, and $K_c{}^2$, may be in error, a circumstance that would yield erroneous conclusions concerning directional asymmetry. These values would be under- or overestimated depending on whether the actual intracellular water volume was larger or smaller than the estimated value, respectively. Significant binding of cationic amino acids to cellular material or compartmentation could

lead to erroneous estimates of the free amino acid levels accessible to the intracellular receptor sites.

REFERENCES

1. Christensen, H. N. (1975) *Biological Transport*, 2nd Ed., pp. 142–144, W.A. Benjamin, Inc., Reading, MA
2. Guidotti, G. G., Borghetti, A. F., and Gazzola, G. C. (1978) *Biochim. Biophys. Acta* **515,** 329–366
3. Baril, E. F., and Potter, V. R. (1968) *J. Nutr.* **95,** 228–237
4. Felig, P. (1975) *Annu. Rev. Biochem.* **44,** 933–955
5. Felig, P., and Wahren, J. (1971) *J. Clin. Invest.* **50,** 2703–2714
6. Owen, E. E., and Robinson, R. R. (1963) *J. Clin. Invest.* **42,** 263–276
7. Schimke, R. T. (1963) *J. Biol. Chem.* **238,** 1012–1018
8. Christensen, H. N. (1977) *Nutr. Rev.* **35,** 129–133
9. White, M. F., Gazzola, G. C., and Christensen, H. N. (1982) *J. Biol. Chem.* **257,** 4443–4449
10. White, M. F., and Christensen, H. N. (1982) *J. Biol. Chem.* **257,** 4450–4457
11. Segel, I. H. (1975) *Enzyme Kinetics*, pp. 534–543, John Wiley & Sons, New York
12. LeFevre, P. G. (1975) in *Curr. Top. Membr. Transp.* **7,** 109–215
13. Devés, R., and Krupka, R. M. (1978) *Biochim. Biophys. Acta* **513,** 156–172
14. Krupka, R. M., and Devés, R. (1981) *J. Biol. Chem.* **256,** 5410–5416
15. Heinz, E. (1972) in *Metabolic Pathways* (Hokin, L. E., ed) Vol. 6, pp. 455–501, Academic Press, New York
16. Christensen, H. N. (1969) *Adv. Enzymol. Relat. Areas Mol. Biol.* **32,** 1–20
17. Christensen, H. N., and Handlogten, M. E. (1979) *J. Neural Transm.* **15,** (suppl.) 1–13
18. Christensen, H. N. (1966) *Fed. Proc.* **25,** 850–853
19. Sly, W. S., and Grubb, J. (1979) *Methods Enzymol.* **58,** 444–450
20. Thompson, E. B. (1979) *Methods Enzymol.* **58,** 544–552
21. Gazzola, G. C., Dall'Asta, V., Franchi-Gazzola, R., and White, M. F. (1981) *Anal. Biochem.* **115,** 368–374
22. Christensen, H. N., and Cullen, A. M. (1973) *Biochim. Biophys. Acta* **298,** 932–850
23. Kurtz, A. C. (1949) *J. Biol. Chem.* **180,** 1253–1267
24. Rognstad, R., and Clark, D. G. (1974) *Arch. Biochem. Biophys.* **161,** 638–646
25. Kletzien, R. F., Pariza, M. W., Becker, J. E., and Potter, V. R. (1975) *Anal. Biochem.* **68,** 537–544
26. Cleland, W. W. (1979) *Methods Enzymol.* **63A,** 103–138
27. Christensen, H. N., and Handlogten, M. E. (1975) *Proc. Natl. Acad. Sci. U. S. A.* **72,** 23–27
28. Christensen, H. N., Handlogten, M. E., Lam, I., Tager, H. S., and Zand, R. (1969) *J. Biol. Chem.* **244,** 1510–1520
29. Gazzola, G. C., Dall'Asta, V., and Guidotti, G. G. (1980) *J. Biol. Chem.* **255,** 929–936
30. Christensen, H. N., and Liang, M. (1966) *J. Biol. Chem.* **241,** 5542–5551
31. Christensen, H. N. (1973) in *Membrane Structure and Mechanisms of Biological Energy Transductions* (Avery, J., ed) pp. 233–263, Plenum Press, London
32. Lieb, W. R., and Stein, W. D. (1974) *Biochim. Biophys. Acta* **373,** 178–196
33. Rosenberg, L. E., and Scriver, C. R. (1980) in *Metabolic Control and Disease* (Bondy, P. K., and Rosenberg, L. E., eds) 8th Ed., p. 633, W.B. Saunders Co., Philadelphia
34. Wilbrandt, W. (1955) *Symp. Soc. Exp. Biol.* **8,** 136–162
35. Karlish, S. J. D., Lieb, W. R., Ram, D., and Stein, W. D. (1972) *Biochim. Biophys. Acta* **255,** 126–132
36. Baker, G. F., and Widdas, W. F. (1973) *J. Physiol. (Lond).* **231,** 143–165
37. Baker, G. F., Basketter, D. A., and Widdas, W. F. (1978) *J. Physiol. (Lond.)* **278,** 377–388
38. Geck, P. (1971) *Biochim. Biophys. Acta* **241,** 462–472
39. Bloch, R. (1974) *J. Biol. Chem.* **249,** 3543–3550
40. Whitesell, R. R., Tarpley, H. L., and Regen, D. M. (1977) *Arch. Biochem. Biophys.* **181,** 596–602
41. Regen, D. M., and Morgan, H. E. (1964) *Biochim. Biophys. Acta* **79,** 151–166
42. Craik, J. D., and Elliot, K. R. F. (1979) *Biochem. J.* **182,** 503–508
43. Graff, J. C., Wohlhueter, R. M., and Plagemann, P. G. W. (1981) *Biochim. Biophys. Acta* **641,** 320–333
44. Plagemann, P. G. W., Wohlheuter, R. M., Graff, J., Erbe, J., and Wilkie, P. (1981) *J. Biol. Chem.* **256,** 2835–2842
45. Taylor, L. P., and Holman, G. D. (1981) *Biochim. Biophys. Acta* **642,** 325–335
46. Hoare, D. G. (1972) *J. Physiol. (Lond.)* **221,** 331–348
47. Vidaver, G. A., and Shepherd, S. L. (1968) *J. Biol. Chem.* **243,** 6140–6150
48. Rosenberg, R. (1981) *Biochim. Biophys. Acta* **649,** 262–268
49. Eavenson, E., and Christensen, H. N. (1967) *J. Biol. Chem.* **242,** 5386–5396
50. Villereal, M. L., and Cook, J. S. (1978) *J. Biol. Chem.* **253,** 8257–8262
51. Laris, P. C., Bootman, M., Pershadsingh, H. A., and Johnstone, R. M. (1978) *Biochim. Biophys. Acta* **512,** 397–414
52. Johnstone, R. M., and Laris, P. C. (1980) *Biochim. Biophys. Acta* **599,** 715–730
53. Turner, R. J. (1981) *Biochim. Biophys. Acta* **649,** 269–280
54. Akedo, A., and Christensen, H. N. (1962) *J. Biol. Chem.* **237,** 118–122
55. Christensen, H. N., and Liang, M. J. (1966) *J. Biol. Chem.* **241,** 5552–5556
56. Christensen, H. N., and Handlogten, M. E. (1968) *J. Biol. Chem.* **243,** 5428–5438

Additional references are found on p. 10080.

Supplementary Material to

The Two-Way Flux of Cationic Amino Acids
Across the Plasma Membrane of Mammalian Cells is Largely
Explained by a Single Transport System

by

Morris F. White and Halvor N. Christensen

In general, nonmechanistic terms, membrane transport of a single substrate such as arginine, by a transport system apparently composed of a single substrate binding site, $\bar{T}$, can be described by steady-state kinetics as the *iso uni uni* reaction sequence (11) diagrammed in Fig. 1. The *iso uni uni* reaction applied to the simple carrier (32) requires that the binding site alternate between two aqueous compartments so that it is available to a substrate in only one compartment at a time. Conversion of the substrate-mediator complex, $S{\bullet}\bar{T}$, into intermediate orientations has been disregarded here because the steady-state approach cannot resolve these hypothetical complexes (57,58). Although a single binding site exposed simultaneously at both sufaces will not yield *iso uni uni* kinetics (59) an arrangement of successive identical binding sites could under certain circumstances do so (60,61). The term "carrier" is used broadly to designate the membrane components which react according to the *iso uni uni* kinetic pathway (Fig. 1), forming an intermolecular complex with a substrate separately at each interface but coupled through conformational or orientational changes. Hence this term does not necessarily imply that a single carrier molecule makes a transmembrane excursion all the way across the plasma membrane to move the bound substrate.

Standard methods (62) or computer assisted analysis (63) for deriving steady-state rate equations applied to the pathway of substrate in Fig. 1 shows that the net influx, $N_{1\to2}$ of S_1 from side 1 (outside) to side 2 (inside) is described by

$$N_{1\to2} = \frac{V^1_{max}{\bullet}[S_1]{\bullet}([S_1] - [S_2]/K_{eq})}{K^1_m(1 + [S_2]/K^2_m) + [S_1](1 + [S_2]/K^2_v)} \tag{4}$$

In the absence of intracellular substrate, S_2, this equation reduces to the familiar Michaelis-Menten expression. The analogous relation shown in Eq. 5 describes solute efflux and is obtained by interchanging the numerical subscripts in Eq. 4 so as to describe the net outward movement of intracellular substrate instead:

$$N_{2\to1} = \frac{V^2_{max}{\bullet}[S_2]{\bullet}([S_2] - [S_1]{\bullet}K_{eq})}{K^2_m(1 + [S_1]/K^1_m) + [S_2](1 + [S_1]/K^1_v)} \tag{5}$$

The experimental significance of these kinetic constants, the corresponding ratios of the molecular rate constants from the scheme in Fig. 1, some useful kinetic identities, and the equivalent terms using Stein's nomenclature (32) are provided in Table 1. Schachter (64) and Segel (11,65) obtained equations identical to Eq. 4 and 5 for a model formally including the interconversion step between the two substrate-carrier complexes, $S_1\bar{T}_1 \rightleftharpoons S_2\bar{T}_2$. Leib and Stein demonstrated that the only difference between the composition of the kinetic parameters for the one- and two-complex representation of the *iso uni uni* reaction lies in the inclusion of two additional molecular rate constants (32).

Measurement of the unidirectional fluxes, V, of radioactively labeled substrates S^*_1 and S^*_2, rather than the net fluxes, N, is a sensitive method usually used for the discrimination of multiple transport systems. The equations describing influx, $V_{1\to2}$, of S^*_1 in the presence of unlabeled S_2, or efflux, $V_{2\to1}$, of S^*_2 in the presence of unlabeled S_1 are obtained by analyzing the complete reaction scheme (Fig. 1) including the path of radioactively labeled (*) and unlabeled substrates as outlined by Schachter (64). Modification of Eq. 4 and 5 using Cleland's rules for isotope exchange yields the same results (62,66). The expressions for the unidirectional fluxes of labeled substrate, the influx (Eq. 6) and the efflux (Eq. 7), are provided below:

$$V_{1\to2} = \frac{V^1_{max}{\bullet}[S_1]{\bullet}(1 + [S_2]/K^2_c)}{K^1_m(1 + [S_2]/K^2_m) + [S_1](1 + [S_2]/K^2_v)} \tag{6}$$

$$V_{2\to1} = \frac{V^2_{max}{\bullet}[S_2]{\bullet}(1 + [S_1]/K^1_c)}{K^2_m(1 + [S_1]/K^1_m) + [S_2](1 + [S_1]/K^1_v)} \tag{7}$$

According to the model in Fig. 1, the observed kinetic parameters for influx, $1/V^1_{obs}$ and K^1_{obs}/V^1_{obs}, are dependent hyperbolically on the intracellular substrate concentration. The relative values of the intracellular Michaelis Constants, K^2_m, K^2_v, and K^2_c, predict the shape of the observed influx curves according to the following relations:

$$(V^1_{obs})^{-1} = \frac{1}{V^1_{max}}\left(\frac{(1 + [S_2]/K^2_v)}{(1 + [S_2]/K^2_c)}\right) \tag{8a}$$

$$\left(\Delta\frac{1}{V^1_{obs}}\right)^{-1} = \frac{V^1_{max}}{(1 - K^2_c/K^2_v)}\left(\frac{K^2_c}{[S_2]} + 1\right) \tag{8b}$$

$$K^1_{obs}/V^1_{obs} = \frac{K^1_m}{V^1_{max}}\left(\frac{(1 + [S_2]/K^2_m)}{(1 + [S_2]/K^2_c)}\right) \tag{9a}$$

$$\left(\Delta\frac{K^1_{obs}}{V^1_{obs}}\right)^{-1} = \frac{V^1_{max}}{K^1_m(1 - K^2_c/K^2_m)}\left(\frac{K^2_c}{[S_2]} + 1\right) \tag{9b}$$

Eq. 8b and 9b are linear transformations of Eq. 8a and 9a, respectively. The values of $(\Delta 1/V^1_{obs})^{-1}$ and $(\Delta K^1_{obs}/V^1_{obs})^{-1}$ are the absolute differences between the values measured in the absence and presence of intracellular substrate. Stimulation of V^1_{obs} and V^1_{obs}/K^1_{obs} occurs when $K^2_c < K^2_v$ and $K^2_c < K^2_m$, respectively; *trans*-inhibition will be observed if these inequalities have the opposite sense.

Four possible turnover numbers describing a complete cycle of the carrier flux in certain limiting circumstances can be defined (31):

1. V^1_{max}: The carrier is saturated with substrate during influx and empty during efflux (zero-*trans* influx).
2. V^2_{max}: The carrier is saturated with substrate during efflux and empty during influx (zero-*trans* efflux).
3. V^{ss}_{max}: The carrier is saturated with substrate during influx and efflux (steady-state or infinite-*trans* flux).
4. V^{oo}_{max}: The carrier is empty during influx and efflux (empty carrier flux).

Examination of the relations in Table 1 verifies that these parameters are related by Eq 10a.

$$\frac{1}{V^1_{max}} + \frac{1}{V^2_{max}} = \frac{1}{V^{ss}_{max}} + \frac{1}{V^{oo}_{max}} \tag{10a}$$

In the special case where $V^1_{max} = V^2_{max}$, the following relation is valid

$$1/V^{oo}_{max} = 2(1/V^1_{max} - 1/2V^{ss}_{max}) \tag{10b}$$

Accumulation of a solute against its concentration gradient requires the net influx, $N_{1\to2}$, to be greater than zero when $[S_1] = [S_2]$. This situation occurs when

$$K_{eq} = \frac{K^2_m{\bullet}V^1_{max}}{K^1_m{\bullet}V^2_{max}} = \frac{k_1k_3k_5}{k_2k_4k_6} = \frac{K^2_c}{K^1_c} > 1 \tag{11a}$$

The apparent accumulation of a charged substrate may represent an electrochemical equilibrium (32) such that

$$K_{eq} = \exp(-\Delta\Psi F/RT) \tag{11b}$$

where $\Delta\Psi$ represents the transmembrane potential, negative inside, and F/RT has a value of 0.034 mV^{-1} at 37C. The uphill transport of nutrients into cells may be more directly coupled to metabolic energy. In this latter case, the simple carrier model is not complete because it does not account explicitly for coupling of transport to other osmotic or chemical gradients. For example, if the binding of S_1 to $\bar{T}_1$ is energy-dependent, k_1 would increase on access to energy; if reorientation of the $\bar{T}_1{\bullet}S_1$ complex and subsequent release of S_2 is energy-dependent, k_3 would be larger when coupled to an energy source (67). The distribution ratio determined from Eq. 11a is theoretically independent of the extracellular substrate concentration. For most cases examined so far, the ratio $[S_2]/[S_1]$ has been found to decrease as $[S_1]$ increases (Fig. 4). This discrepancy can be resolved by assuming that compartmental leaks become conspicuous at high substrate concentrations or that the energy, whether a membrane potential or something else, is disipated at high levels. Within a physiological concentration range where anomalies remain minor, the *iso uni uni* reaction describes uphill transport and countertransport in a useful way.

Some approximations (32) based on Eq. 6 and 7 are used in this report to interpret cationic amino acid transport:

1. *Zero-trans influx*

   Assumption: $[S_2] = 0$; $[S^*_1]$ is variable

$$V_{1\to2} = \frac{V^1_{max}{\bullet}[S^*_1]}{K^1_m + [S^*_1]} \tag{12}$$

2. *Zero-trans efflux*

   Assumption: $[S^*_2]$ is variable; $[S_1] = 0$

$$V_{2\to1} = \frac{V^2_{max}{\bullet}[S^*_2]}{K^2_m + [S^*_2]} \tag{13}$$

3. *Infinite-trans influx*

   Assumption: $[S_2]$ is infinite; $[S^*_1]$ is variable

$$V_{1\to2} = \frac{V^1_{max}{\bullet}K^2_v/K^2_c{\bullet}[S^*_1]}{K^1_m{\bullet}K^2_v/K^2_m + [S^*_1]} \tag{14a}$$

$$= \frac{V^{ss}_{max}{\bullet}[S^*_1]}{K^1_v + [S^*_1]} \tag{14b}$$

4. *Infinite-trans efflux*

   Assumption: $[S^*_2]$ is variable; $[S_1]$ is infinite

$$V_{2\to1} = \frac{V^2_{max}{\bullet}K^1_v/K^1_c{\bullet}[S^*_2]}{K^2_m{\bullet}K^1_v/K^1_m + [S^*_2]} \tag{15a}$$

$$= \frac{V^{ss}_{max}{\bullet}[S^*_2]}{K^2_v + [S^*_2]} \tag{15b}$$

5. *Steady-state influx*

Assumption: $[S_2] = [S_1^*] \cdot K_{eq}$

$$v_{1\to2} = \frac{V^1_{max} \cdot K_v^2/K_c^2 \cdot [S_1^*]}{K_m^1 \cdot K_v^2/K_c^2 + [S_1^*]} \quad (16a)$$

$$= \frac{V^{ss}_{max} \cdot [S_1^*]}{K_s^1 + [S_1^*]} \quad (16b)$$

6. *First-order efflux*

Assumption: $[S_2^*] \ll K_m^2$; $[S_1]$ is variable

$$\frac{[S_2^*]}{v_{2\to1}} = \frac{K_m^2}{V^2_{max}} \left(\frac{(1 + [S_1]/K_m^1)}{(1 + [S_1]/K_c^1)} \right) \quad (17a)$$

and the linear transformation

$$\left(\Delta \frac{[S_2^*]}{v_{2\to1}} \right)^{-1} = \frac{V^2_{max}}{K_m^2(1 - K_c^1/K_m^1)} \left(\frac{K_1}{[S_1]} + 1 \right) \quad (17b)$$

where $1/\Delta([S_2^*]/v_{2\to1})$ is the reciprocal of the absolute difference between the values of $[S_2^*]/v_{2\to1}$ measured in the absence and presence of S_1. The value of $v_{2\to1}/[S_2^*]$ is approximately equal to V^2_{max}/K_m^2 when $[S_1]$ is zero, whereas it is equal to V^{ss}_{max}/K_v^2 when $[S_1]$ is infinite.

Supplementary References

57. Stein, W. D., and Honig, B. (1977) Mol. Cell. Biochem. *15*, 27-44
58. Cleland, W. W. (1963) Biochim. Biophys. Acta *67*, 104-137
59. Lieb, W. R., and Stein, W. D. (1974) Biochim. Biophys. Acta *373*, 165-177
60. Devès, R. and Krupka, R. M. (1978) Biochim. Biophys. Acta *513*, 156-172
61. Krupka, R. M., and Devès, R. (1981) J. Biol. Chem. *256*, 5410-5416
62. Huang, C. Y. (1979) in Meth. in Enzymol. (Purich, D. L., ed.) Vol. 63A, pp. 54-84, Academic Press, New York
63. Fromm, H. J. (1979) in Meth. in Enzymol. (Purich, D. L., ed.) Vol. 63A, pp. 84-103, Academic Press, New York
64. Schachter, H. (1972) in Metabolic Pathways (Hokin, L. E., ed.) 3rd Ed., Vol. 6, pp. 1-15, Academic Press Inc., New York
65. Cuppoletti, J., and Segel, I. H. (1974) J. Membrane Biol. *17*, 239-252
66. Cleland, W. W. (1975) Biochemistry *14*, 3220-3224
67. Kotyk, A. (1973) Biochim. Biophys. Acta *300*, 183-210